Magnesium Technology 2013
Edited by: Norbert Hort, Suveen N. Mathaudhu, Neale R. Neelameggham, and Martyn Alderman
TMS (The Minerals, Metals & Materials Society), 2013

INFLUENCE OF YTTRIUM ON CREEP BEHAVIOR IN NANO-CRYSTALLINE MAGNESIUM USING MOLECULAR DYNAMICS SIMULATION

M. A. Bhatia[1], K.N. Solanki[1]
[1]School of Energy, Matter and Transport; Arizona State University; Tempe, AZ 85287-6106, USA

Keywords: Magnesium, Yttrium, Creep, Creep rate, Grain boundary

Abstract

Due to their light weight, magnesium (Mg) and its alloys have great potential for reducing vehicular mass and energy consumption. However, the use of Mg alloys is currently restricted to low-temperature automotive components application. This work strives to gain a better understanding of the effect of yttrium (Y) (up to 3at%) on creep behavior of columnar nanocrystalline Mg with a grain size of 5nm and 10nm. Using molecular dynamics (MD) simulations, nanocrystalline Mg with various local concentrations of Y was subjected to a constant-stress loading, ranging from 0-500MPa, at different initial temperatures, ranging from 473-723K. Our simulations reveal that the secondary stage creep rate ($\dot{\varepsilon}$) decreases by 71% with the addition of only 1at% Y at 500MPa and 623K. With the addition of alloying elements such as Y, the creep rate in the secondary region decreases and the creep deformation mechanism is changed from the void nucleation, growth, and coalescence to GB rotation/sliding. The analyses of the diffusion coefficient and energy barrier reveal a stronger contribution to the overall deformation by the grain boundary diffusion at the low-temperature (423K) and by the lattice diffusion at the higher-temperature (723K).

Introduction

Increasing global demand for energy-efficient yet safer material requires development of new lightweight alloys. Among structural materials, Magnesium (Mg) has the highest strength-to-weight ratio. Moreover, Mg-alloys have excellent recyclability and are ideal for transportation and biological material applications, with enormous potential for energy savings [1-4]. However, Mg has certain limitations when compared with other metallic systems and polymers [5]. Since Mg has a hexagonal close packed (hcp) structure, it has a limited number of active slip systems at room temperature [6-7], which leads to failure in polycrystalline Mg-alloys at ambient conditions before dislocation glide can occur [8-9]. In an effort to overcome this material performance shortcoming, recent studies have considered the effects of adding to Mg certain alloying elements, such as Al-Zn, Al-Si, Al-Ca, Al-Sr, Sn-Ca, Zr-Y, and minute traces of other rare-earth (RE) elements. The objective of these studies has been to qualitatively identify the principles governing solute strengthening and ductility while improving manufacturability as well as lowering production costs of these alloys (e.g., [10-11]). These studies have shown that the alloying elements can cause Mg-alloys to either harden or soften by interacting with dislocations/twins/interface and/or forming favorable phases [10]. Rare earth elements in particular have been found to generate the most favorable effects on the mechanical and physical properties of Mg-alloys, including improved creep and corrosion resistances [10, 16]. However addition of RE is cost prohibitive [12], so other alternatives are needed. In order to develop additional, cost-effective alloys, a better understanding of the deformation mechanisms governing Mg-alloys' performance is necessary.

The high-temperature deformation mechanisms, such as creep in metallic systems, have been extensively studied over the years, and for a detailed review, please refer to [14]. In fact, it is a well-established fact that with increasing temperature, creep reduces the load-bearing capacity of Mg-alloys. During creep, the strain is accumulated either by diffusional flow through the interfaces (Nabarro-Herring creep [22], [23]), diffusional flow along interfaces (Coble creep [27]), interface sliding (Raj and Ashby [24]), or dislocation motion (climb/glide [25]). In general, these creep mechanisms/models have been vigorously discussed as well (e.g., see [14]), mostly due to the inability of certain models to accurately predict creep behavior across materials with varying microstructures. In a recent experimental study, it has been shown that microstructural attributes such as grain size and solutes/phases segregated to the grain boundary (GB) play an important role in creep behavior of Mg-alloys [26]. It was found that with increasing grain size, the creep rate decreased with an attendant loss in room temperature yield strength, as predicted by the Hall-Petch equation [25]. On the other hand, grain-size refinement can be controlled by the addition of micro-alloys, such as Zr [26]. Thus, with a balance between goals for optimal grain size and room-temperature strength, creep deformation behavior potentially could be enhanced by elucidating the deformation mechanisms necessary to engineer GBs with solutes such as yttrium (Y).

In this paper, extensive MD simulation results are presented to elucidate the effect of grain size (5nm-15nm) and GB with various Y concentrations (1-3%at) on diffusional creep and deformation mechanism of nanocrystalline Mg.

Simulation Methodology

A parallel molecular dynamics code (LAMMPS) [18] that incorporates spatial decomposition was used to deform the nanocrystalline Mg samples of 5nm-15nm grain dimension as shown in Fig 1. The Voronoi tessellation method [21] was used to construct $[11\bar{2}0]$ columnar samples containing 5 grains of identical hexagonal shape within periodic simulation cells. After generating the desired Mg nanocrystalline model, the GB of the model was locally doped with different (1~3%at) percentages of Y. The total number of atoms in a simulation cell was in the range of 250000-1 million. The samples were first relaxed at the desired temperature using an NVT (conserving number of atoms, volume and temperature) ensemble for 15 ns, followed by an independent relaxation in three directions using an NPT (conserving number of atoms, pressure and temperature to mimic bulk behavior) ensemble for another 10 ns. Atomistic simulations were carried out using an MD time step of 1 fs. A periodic boundary condition was adopted in all directions. A constant stress, ranging from 0-500MPa, was applied along y-direction at different temperatures ranging from 423k – 723k (150 °C – 450 °C), whereas deformation in the other two directions was carried out by

maintaining a zero pressure according to the Parrinello-Rahman method [19].

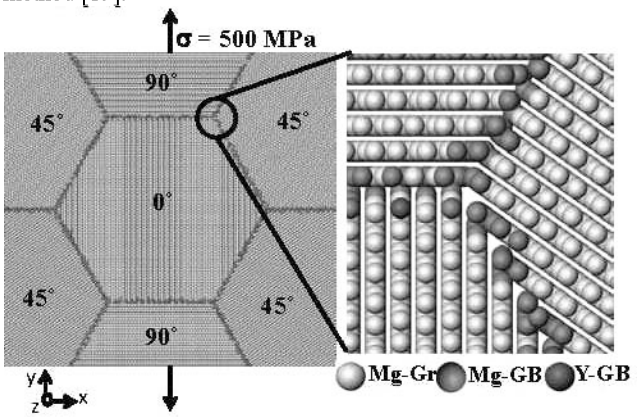

Fig 1 a) An equilibrated, undeformed simulation model at 473K with different misorientation angles with respect to the loading (y) direction. Viewing direction is along the $[11\bar{2}0]$ columnar z-axis. b) Triple point showing Mg lattice atoms (yellow), Mg GB atoms (Red), and doped Y atoms (blue).

The molecular dynamics simulations in this work employed the embedded atom method (EAM) potential of Sheng [20]. The interatomic potential parameters were derived from a fitting method using isothermal compressibility data up to 2000 K (1727 ˚C). Moreover, the potential was developed by also fitting the vacancy migration energy as well as with different Mg-Y crystal structures. It is important to note here that a recent study [21] that investigated the effect of precipitate in aluminum alloys proposed that thermally-activated vacancy movement plays a central role in grain growth mechanism.

Results and Discussions

Diffusional analysis with varying grain sizes at 0 MPa

To study the diffusional mechanisms of nanocrystalline Mg, equilibrated structure with different grain sizes were annealed for 500 ps in the temperature range of 473 K – 723 K under zero applied load condition. These simulations were used to calculate the mean square displacement (MSD) values as

$$MSD = \sum_{i=1}^{N} (r_i(t) - r_i(0))^2$$

at different constant temperatures, where N is the number of atoms, $r_i(t)$ is the position of an atom at any instant t, and $r_i(0)$ is the initial position of an atom at t=0. From the MSD values, we computed the diffusion coefficient with the help of Einstein's equation as follows:

$$MSD = 6Dt,$$

where D is the diffusion coefficient, and t is the time. Figure 2 shows Arrhenius plots for self-diffusion of Mg atoms in nanocrystalline Mg with different grain sizes that are given by following:

$$D = D_o e^{-Q/KT},$$

where D_o is the maximum diffusion coefficient at infinite temperature, Q is the activation energy, K is the Boltzmann constant, and T is the temperature.

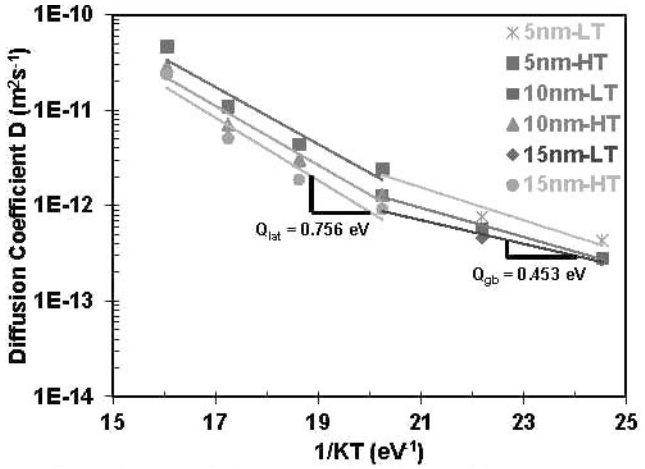

Fig 2 Arrhenius plots for self-diffusion of Mg atoms in nanocrystalline Mg with different grain sizes showing two distinct slopes corresponding to the lattice (at high temperature) and GB diffusions (at low temperature). The transition temperature from the GB-dominant to lattice-dominant diffusion mechanism was found to be at 573K. LT – Low Temperature HT- High Temperature

As the grain size increases, the activation energy for GB diffusion and for lattice diffusion increases. Table 1 lists the respective activation energies for nanocrystalline Mg with different grain sizes. It is to be noted that the fraction of GB atoms increases as the grain size decreases. Hence, with smaller grain sizes, the contribution from the GB diffusion increases and dominates the creep deformation mechanism as predicted by the activation energy ratio $Q_R = Q_{gb}/Q_{lattice}$, where Q_{gb} is the GB diffusion activation energy, and Q_{gb} is the lattice diffusion activation energy. For the nanocrystalline Mg with 5nm grain size, Q_R is equal to 0.558 and hence the activation energy of GB diffusion (0.384 eV) is much lower than activation energy of lattice diffusion (0.688 eV). As the grain size increases, the activation energy also increases, but the rate of increase in activation energy for the lattice diffusion is slower than for the GB diffusion. Moreover, the fraction of GB atoms' contribution to total diffusion also decreases. Hence, at 15nm grain size, Q_R is equal to 0.599. Further work is required to find out the grain size at which there is a transition from the GB diffusion to the lattice diffusion mechanism.

Table 1. Activation energies of the GB diffusion and the lattice diffusion in Mg nanocrystalline with different grain sizes. $Q_R = Q_{gb}/Q_{lattice}$ is the parameter used to identify dominant diffusional mechanisms. A smaller ratio indicates less activation energy for GB diffusion, and GBD dominates.

Grain Size	Fraction of GB atoms	Lattice diffusion	GB diffusion	Ratio
	f_{gb}	Q_{lat} (eV)	Q_{gb} (eV)	Q_R
5nm	0.03528	0.688	0.384	0.558
10nm	0.02465	0.714	0.413	0.578
15nm	0.02013	0.756	0.453	0.599

Diffusional analysis with varying concentrations of Yttrium at 0 MPa

To monitor the diffusion paths of the GB atoms, the equilibrated 5nm grain nanocrystalline structure with different initial concentration of Y was annealed for 250 ps under zero applied stress in the temperature range 423–723 K. These equilibrated structures were used to calculate mean square displacement (MSD) at given temperatures of interest. Figure 3 shows the MSD evolutions for the Mg and Y atoms for different temperatures. These results suggest a linear increase in MSD values for both Mg and Y, with Mg being more mobile than Y.

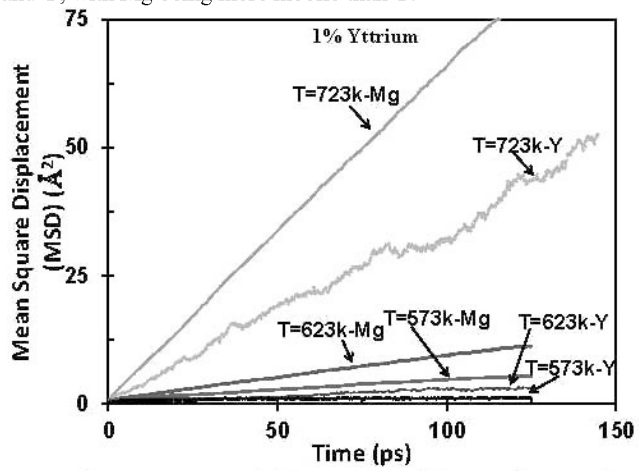

Fig 3 The mean square displacement evolutions of Mg and Y atoms for a 5nm grain size Mg-1%Y nanocrystalline at different temperatures in the absence of external stress loading. These results suggest a linear increase in MSD values for both Mg and Y, with Mg being more mobile than Y.

Figure 4 shows the Arrhenius plots for self-diffusivity of Mg and Y in 5nm-grain size Mg-1%Y nanocrystalline sample. In the case of Mg-1%Y, for a low temperature range, the self-diffusivity activation energy of Y, 0.094 eV, is lower than that of Mg, 0.279 eV. In contrast, for a higher temperature range, the self-diffusivity activation energy of Y, 0.93 eV, is higher than that of Mg, 0.659 eV. However, in the case of Mg-3%Y, for high temperature, the self-diffusivity activation energy of Mg and Y decreases when compared with Mg-1%Y. Table 2 lists the respective self-diffusivity activation energies of Mg and Y in Mg nanocrystalline with different Y concentrations.

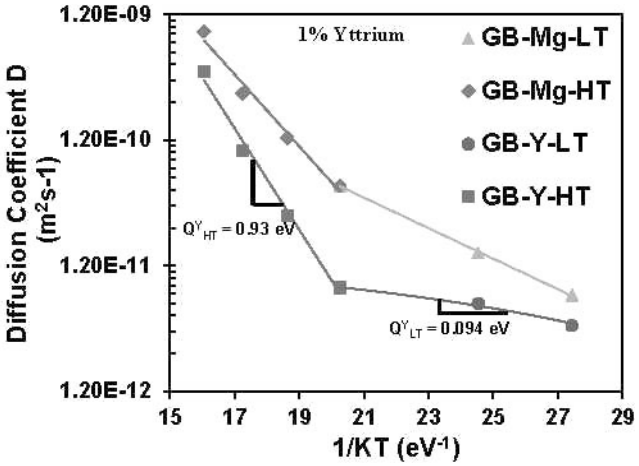

Fig 4 Arrhenius plots for self-diffusive GB Mg and Y atoms in a 5nm-grain size Mg-1%Y nanocrystalline sample. At lower temperature, the activation energy of Y, 0.094 eV, is lower than that of Mg, 0.279 eV. In contrast, at higher temperature, the activation energy of Y, 0.93 eV, is higher than that of Mg, 0.659 eV.

Table 2 The respective self-diffusivity activation energies of Mg and Y in Mg nanocrystalline with different Y concentrations.

Activation Energy Q (eV)			
	0% at. Y	**1% at. Y**	**3% at. Y**
Mg-GB LT	0.180	0.279	0.340
Mg-GB HT	0.593	0.659	0.588
Y-GB LT		0.094	0.180
Y-GB HT		0.930	0.894

Diffusional analysis with varying grain sizes at 500 MPa

To study the effect of applied loads, a constant applied stress of 500 MPa was applied in a y-direction, and lateral dimensions were held at 0 MPa. The magnitude of the applied stress was low enough to ensure that no dislocations were nucleated from the GBs. Figure 5 shows the strain as a function of time at 623 K with different grain sizes. Creep behavior in Figure 5 is divided into three regions, which is observed in many materials. In Region I (primary creep), there is an instantaneous response, followed by a decreasing rate of strain with increase in time. In Region II (secondary creep), the strain increases linearly with time. In Region III (tertiary creep), the strain increases rapidly with time. Most of the damage or fracture is experimentally observed in Region III due to voids and crack nucleations. We also observe, as shown in Figure 5, that the secondary creep in the 5nm-grain sample is short-lived in comparison to the 10nm- and 15nm-grain nanocrystalline samples. Based on these results, we used the 10nm-grain nanocrystalline sample to further explore the effect of Y on the steady state creep regime. Our main objective here was to determine whether alloying elements such as Y can delay tertiary creep by prolonging the secondary creep regime.

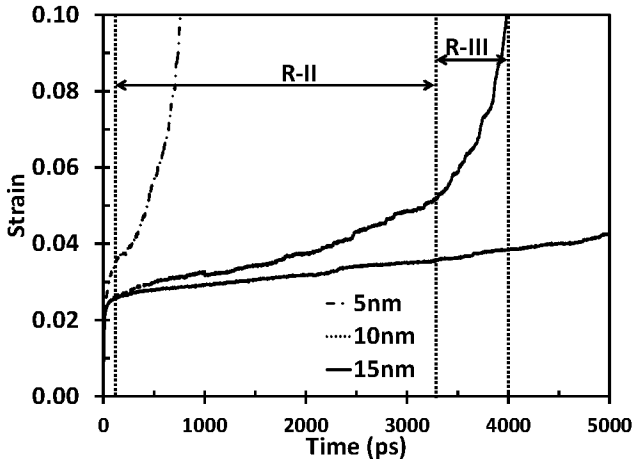

Fig 5 Total strain as a function of time for different grain sizes at 623 K temperature with a constant applied stress of 500 MPa. After initial elastic region, the secondary creep regime (R-II) for

5nm-grain exists for about 200 ps. In contrast, for the 10nm-grain, Region II exists for a longer period (3800 ps) of time. Figure shows R-II and R-III for 10nm grain.

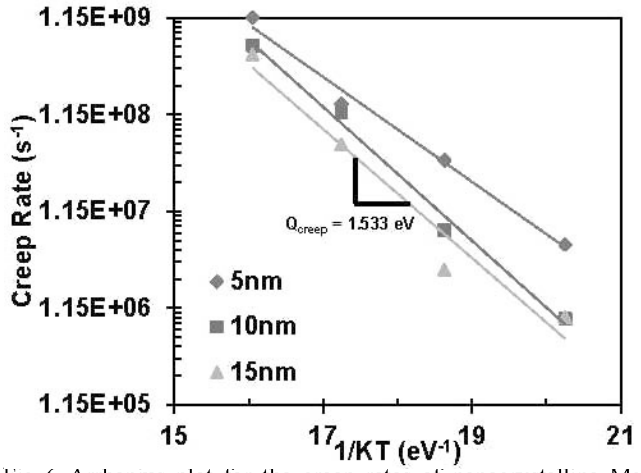

Fig 6 Arrhenius plot for the creep rates of nanocrystalline Mg with different grain sizes. The creep activation energy for 5nm- and 15nm-grain sizes was found to be 1.047 eV and 1.533 eV, respectively.

An empirical equation which describes the strain-time relation is given by

$$\dot{\varepsilon} = \frac{C\sigma^m}{d^b} e^{-Q/KT}$$

where C, m, and d are material constants, $\dot{\varepsilon}$ is the secondary creep rate, σ is the applied stress, d is the mean grain size, Q is the creep activation energy. Figure 6 shows an Arrhenius plot for the secondary creep rates of nanocrystalline Mg with different grain sizes for a temperature range 573–723 K. The increase in the creep rate with increasing temperature indicates that the deformation is thermally activated, indicative of a diffusion-driven creep mechanism. The creep activation for 5nm- and 15nm-grain sizes was found to be 1.047 eV (101 kJ/mol) and 1.533 eV (148 kJ/mol), respectively, which are in good agreement with the experimental range of 106–220 kJ/mol reported in literature [10] for different applied stresses and temperature ranges.

Diffusional analysis with varying concentrations of Yttrium at 500 MPa

Figure 7 shows strain as a function of time for a 10nm-grain nanocrystalline sample with different concentrations of Y at 673K and with an applied constant stress of 500MPa. Initially, for the pure Mg nanocrystalline sample, we observed that the material deformed elastically until t = 20 ps. Thereafter, the strain increases linearly at a constant creep rate, as shown in Figure 7. In the tertiary creep region (R-III), there is sudden increase in the strain rate that results in nucleation of cracks and voids, leading into an intergranular fracture as shown in Figure 8a. With the addition of alloying elements such as Y, the creep rate in the secondary region (R-II) decreases, indicative of GB stabilizations, as shown in Figures 8b and 8c. Moreover, with the addition of Y, the creep deformation mechanism is changed from void growth and coalescence to grain shrinkage and rotation, as shown in Figure 8. Further work is required to study grain rotation and stretch at different concentrations of Y to enhance our understanding of Y's effect on creep behavior as it is shown in Figure 8. Note that the creep rate for the tertiary creep region with 1% Y is lower than that for 2% and 3%at Y, as seen in Figures 7 and 9. Finally, Figure 9 shows an Arrhenius plot for the creep rates of nanocrystalline Mg with different concentrations of Y for a range of temperatures 573–723 K. We observe a slight change in the overall creep rate, with creep activation energy increasing from 1.128-1.154 eV for 0-3% at Y as shown in Figure 9.

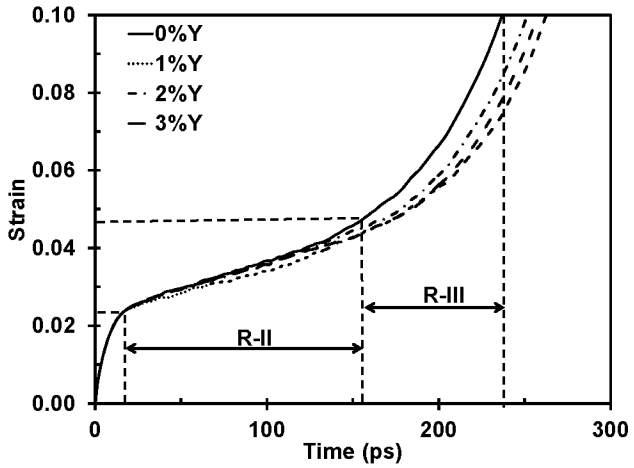

Fig 7 Total strain as a function of time for a 10nm-grain nanocrystalline sample with different concentrations of Y at 673 K and an applied constant stress of 500 MPa. After the initial elastic region, the creep rate decreases to a steady state that persists throughout the secondary creep region (R-II), where small voids are formed in the pure Mg polycrystalline model. In the tertiary creep region (R-III), the creep rate increases, resulting in an intergranular fracture in the pure Mg nanocrystalline sample. Figure shows R-II and R-III for 0% Yttrium sample.

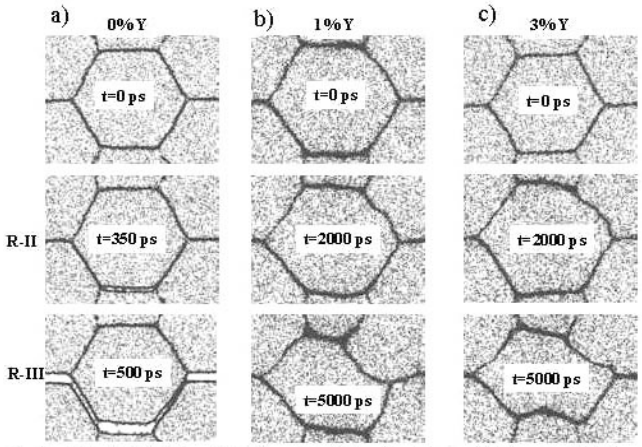

Fig 8 Snapshot showing the variation in microstructure under a constant stress of 500 MPa and at 623 K temperature. a) Micro cracks are formed in the pure Mg nanocrystalline model in the R-II region (secondary creep) at GB, which coalesces in the R-III region (tertiary creep), resulting in an inter-granular fracture due to thermal stresses. For b) and c), no nano-cracks were formed at the GB in the R-II region, and the deformation proceeds with GB migration where the central grain shrinks in tertiary creep region (R-III). Atoms are filtered with potential energy higher than -1.35 eV.

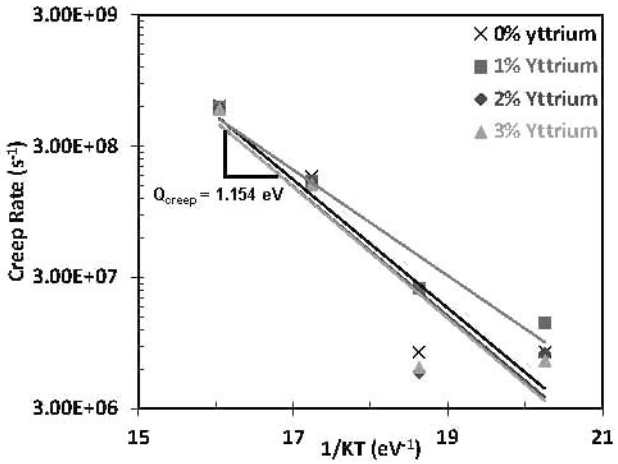

Fig 9 Arrhenius plot for the creep rates of nanocrystalline Mg with different local concentrations of Y. The creep activation energy increases from 1.128-1.154 eV for 0-3% Y.

Conclusion

In this paper, we present the high-temperature deformation behavior and mechanisms of nanocrystalline Mg with and without Y for a temperature range of 573–723 K under constant stress loadings. Our simulations show that with the addition of alloying elements such as Y, the creep rate in the secondary region decreases, indicative of GB stabilizations, as shown in Figures 8b and 8c. Moreover, with the addition of Y, the creep deformation mechanism is changed from void growth and coalescence to grain shrinkage and rotation as shown in Figure 8. The following conclusions can be drawn from this work:

1. For Mg nanocrystalline in the absence of external load, we observed the transition temperature from the GB-dominant to lattice-dominant diffusion mechanism at 573K. Similarly, in the absence of external load for the case of Mg-1%Y, at a lower temperature range, the self-diffusivity activation energy of Y, 0.094 eV, is lower than that of Mg, 0.279 eV. In contrast, for a higher temperature range, the self-diffusivity activation energy of Y, 0.93 eV, is higher than that of Mg, 0.659 eV. However, in the case of Mg-3%Y, for high temperature, the self-diffusivity activation energy of Mg and Y decreases when compare with Mg-1%Y.
2. In the case of constant applied stress of 500MPa on the Mg nanocrystalline sample with different grain sizes, we observe, as shown in Figure 5, that the secondary creep in the 5nm-grain is short lived as compared to 10nm- and 15nm-grain nanocrystalline samples.
3. The creep activation for 5nm- and 15nm-grain sizes in pure Mg nanocrystalline samples was found to be 1.047 eV (101 kJ/mol) and 1.533 eV (148 kJ/mol), respectively, which are in good agreement with the experimental range of 106–220 kJ/mol reported in literature [10] for different applied stresses and temperature ranges.
4. With the addition of alloying elements such as Y, the creep rate in the secondary region decreases and the creep deformation mechanism is changed from the void nucleation, growth, and coalescence to GB rotation/sliding.
5. Finally, further work is required to study grain rotation and stretch at different concentrations of Y to enhance our understanding of Y's effect on creep behavior as seen in Figure 8.

Acknowledgement

The authors are grateful for the financial support for this work from the School for the Engineering of Matter, Transport, and Energy (SEMTE) at Arizona State University. We also appreciate the Fulton High Performance Computing at Arizona State University for enabling us to conduct our simulations.

References

1. S. N. Mathaudhu and E. A. Nyberg, "Magnesium alloys in US military applications: Past, Current and Future Solutions", Magnesium Technology 2010: Proceedings of a Symposium Sponsored by the Magnesium Committee of the Light Metals Division of TMS, 2010.
2. A. A. Luo, "Recent magnesium alloy development for automotive powertrain application", Materials Science Forum, vol. 419-422, pp. 57-66, 2003.
3. K. N. Solanki, A. Moitra, and M. Bhatia, "Effect of substituted aluminum in magnesium tension twin", Magnesium Technology 2010, pp. 325-329, 2010.
4. J. A. Yasi, L. G. Hector Jr., and D. R. Trinkle, "First principles data for solid-solution strengthening of magnesium: From geometry and chemistry to properties", Acta Materialia, vol. 58, no. 17, pp. 5704-5713, Oct. 2010.
5. T. M. Pollock, "Weight loss with magnesium alloys", Science, vol. 328, no. 5981, pp. 986-987, May 2010.
6. J. W. Christian and S. Mahajan, "Deformation twinning", Progress in Materials Science, vol. 39, no. 1–2, pp. 1-157, 1995.
7. A. H. Cottrell and B. A. Bilby, "A mechanism for the growth of deformation twins in crystals", Philosophical Magazine Series 7, vol. 42, no. 329, pp. 573-581, 1951.
8. D. L. McDowell and G. B. Olson, "Concurrent design of hierarchical materials and structures", Scientific Modeling and Simulations, vol. 68, S. Yip and T. D. Rubia, Eds. Dordrecht: Springer Netherlands, 2008, pp. 207-240.
9. W. A. Curtin, D. L. Olmsted, and L. G. Hector, "A predictive mechanism for dynamic strain ageing in aluminum-magnesium alloys", Nature Materials, vol. 5, no. 11, p. 875, Oct. 2006.
10. N. D. Saddock, "Microstructure and creep behavior of Mg-Al alloys containing alkaline and rare earth additions", PhD Dissertation-2008.
11. Y. C. Lee, A. K. Dahle, and D. H. StJohn, "The role of solute in grain refinement of magnesium", Metallurgical and Materials Transactions A, vol. 31, no. 11, pp. 2895-2906, Nov. 2000.
12. S. Agnew, "NSF workshop: Magnesium alloys science and technology-Fundamental research issues", Arlington, Virginia, 2011.
13. V. Vitek and M. Igarashi, "Core structure of 1/3<1120> screw dislocations on basal and prismatic planes in hcp metals: An atomistic study", Philosophical Magazine A, vol. 63, no. 5, pp. 1059-1075, May 1991.
14. H. V. Swygenhoven, "Grain boundaries and dislocations", Science, vol. 296, no. 5565, pp. 66-67, Apr. 2002.

15. M. Tschopp, K. N. Solanki, and M. Horstemeyer, "A generalized framework for quantifying material structure-property relationships and uncertainties: Applicability to ICME", Models, Databases, and Simulation Tools Needed for the Realization of Integrated Computational Materials Engineering: Proceedings of the Symposium Held at Materials Science & Technology 2010, October 18-20, 2010 Houston, Texas, USA, 2011.
16. N. Kashefi, R. Mahmudi, "The microstructure and impression creep behavior of cast AZ80 magnesium alloy with yttrium additions", Materials and Design, vol 39, pp. 200-210, 2012.
17. Tapan G. Desai, Paul C. Millett and Dieter Wolf, "Molecular dynamics study of diffusional creep in nanocrystalline UO2", Acta. Materialia, vol 56, pp. 4489-4497, September 2008.
18. S. J. Plimpton, "Fast parallel algorithm for short-range molecular dynamics", J Comp Phys. vol. 117, pp. 1-19, 1995.
19. M. Parrinello and A. Rahman, "Polymorphic transitions in single crystals: A new molecular dynamics method", J. Appl. Phys. vol. 52, 1981.
20. https://sites.google.com/a/gmu.edu/eam-potential-database/Home/MgY. Manuscript under review.
21. P. S. De, J. Q. Su and R. S. Mishra, "A stress-strain model for a two-phase ultrafine-grained aluminum alloy", Scripta Materialia (2011).
22. F. R. Nabarro, "Deformation of crystals by the motion of single ions", in Report of a conference on strength of solids, held at the HH Wills Physical Laboratory, University of Bristol, on 7-9 July 1947, 1948, p. 75.
23. C. Herring, "diffusional viscosity of a polycrystalline solid", Journal of Applied Physics, vol. 21, no. 5, pp. 437-445, May 1950.
24. R. Raj and M. F. Ashby, "On grain boundary sliding and diffusional creep", Metallurgical Transactions, vol. 2, no. 4, pp. 1113-1127, Apr. 1971.
25. G. E. Dieter, Mechanical metallurgy. McGraw-Hill, 1986.
26. S. M. He, X. Q. Zeng, L. M. Peng, X. Gao, J. F. Nie, and W. J. Ding, "Microstructure and strengthening mechanism of high strength Mg-10Gd-2Y-0.5Zr alloy", Journal of Alloys and Compounds, vol. 427, no. 1–2, pp. 316-323, Jan. 2007.
27. R. L. Coble, "A model for boundary diffusion controlled creep in polycrystalline materials", Journal of Applied Physics, vol. 34, no. 6, pp. 1679-1682, Jun. 1963.